Research Paper

Extracellular histones induce inflammation and senescence of vascular smooth muscle cells by activating the AMPK/FOXO4 signaling pathway

Hang Yang[1], Yong-Yan Luo[2], Lue-Tao Zhang[1], Kai-Ran He[1], Xiao-Jun Lin[1]

[1]Department of Emergency and Critical Care Medicine, Guangdong Provincial People's Hospital, Guangdong Academy of Medical Sciences, Guangzhou, China
[2]Department of Emergency and Critical Care Medicine, Guangdong Provincial People's Hospital ZhuHai Hospital, Zhuhai, China

Correspondence to: Hang Yang; **email:** hangyang_gpph@163.com, https://orcid.org/0000-0003-1637-4499
Keywords: inflammatory response, senescence, VSMC, extracellular histones, organ injury
Received: September 27, 2021 **Accepted:** January 14, 2022 **Published:**

ABSTRACT

Sepsis is an abnormal immune-inflammatory response that is mainly caused by infection. It can lead to life-threatening organ dysfunction and death. Severely damaged tissue cells will release intracellular histones into the circulation as damage-related molecular patterns (DAMPs) to accelerate the systemic immune response. Although various histone-related cytotoxicity mechanisms have been explored, those that affect extracellular histones involved in vascular smooth muscle cell (VSMC) dysfunction are yet to be determined. We found that extracellular histones induced senescence and inflammatory response in a dose-dependent manner in cultured VSMCs. Histone treatment significantly promoted apoptosis-associated speck-like protein containing CARD (ASC) as well as NACHT, LRR and PYD domains-containing protein 3 (NLRP3) interaction of inflammasomes in VSMCs. Forkhead box protein O4 (FOXO4), which is a downstream effector molecule of extracellular histones, was found to be involved in histone-regulated VSMC inflammatory response and senescence. Furthermore, the 5'-AMP-activated protein kinase (AMPK) signaling pathway was confirmed to mediate extracellular histone-induced FOXO4 expression, and blocking this signaling pathway with an inhibitor can suppress vascular inflammation induced by extracellular histones *in vivo* and *in vitro*. These results suggest that the AMPK/FOXO4 pathway is a potential target in treating histone-mediated organ injury.

INTRODUCTION

Sepsis is described as an abnormal immune-inflammatory response that is caused primarily by infection. This condition can lead to life-threatening multiple organ dysfunction syndrome and death [1]. More than 31.5 million people worldwide are threatened with sepsis annually; of them, more than 5.3 million die [2]. In China, more than 20% of patients in the intensive care unit (ICU) develop sepsis, and the mortality rate among these patients is as high as 36% [3]. Despite tremendous efforts made for decades, there is no specific treatment for sepsis [4]. Traditional therapy often ignores the immunopathological nature of sepsis, making it difficult to improve the survival of patients with severe sepsis and septic shock [5]. Vascular smooth muscle cells (VSMCs) are present in the media layer of blood vessels and regulate the tension and contraction of blood vessels [6]. Unlike vascular endothelial cells, the role of VSMCs in sepsis is often overlooked [7]. The increased permeability of endothelial cells in sepsis allows direct contact of VSMCs with inflammatory mediators in the blood, which could lead to disruption of the autoregulation of normal blood vessels [8]. Vascular dysregulation and the toxicity of inflammatory mediators may be

important factors for organ dysfunction [9]. Therefore, controlling the dysregulated immune response and balancing the function of VSMCs should be considered to reduce the incidence of death due to sepsis.

Histones are highly cationic nuclear proteins that are mainly present in the nucleus and participate in chromatin assembly and regulation of gene expression [10]. When cells are exposed to harsh conditions, histones are released into the circulation and serve as damage-related molecular patterns [11]. Circulating histones interact with phospholipids in the cell membrane to mediate distant organ damage [12]. Histones also mediate inflammation, organ damage, and death by activating the Toll-like receptor (TLR) and NACHT, LRR and PYD domains-containing protein 3 (NLRP3) inflammasome pathways [13–15]. Emerging research has shown that extracellular histones play a role in multiple organ damage and death in sepsis [16]. Shi et al. found that lipopolysaccharide (LPS)-induced extracellular histones can cause septic pyrolysis via the NOD2 and VSIG4/NLRP3 pathways [17]. Extracellular histones were found to induce autophagy and apoptosis of human endothelial cells via the mTOR signaling pathway [13]. Circulating histones can cause cerebrovascular damage or brain dysfunction by altering the blood–brain barrier [18]. Although VSMCs play a key role in sepsis [19, 20], the effect of extracellular histones on VSMCs in organ injury remains unclear.

Previous research found that extracellular histones are cytotoxic to endothelial cells [13]. However, if extracellular histones are also cytotoxic to VSMCs, they may lead to cell responses that might worsen the disease. Thus, elucidating the mechanism underlying histone-mediated cytotoxicity could aid in understanding the complex pathogenesis of organ injury. In this study, we found that extracellular histones facilitate VSMC senescence and inflammation in a dose-dependent manner. In addition, Forkhead box protein O4 (FOXO4), a downstream histone regulator, was found to be involved in histone-regulated VSMC inflammation and senescence. Mechanically, the AMPK signaling pathway mediates extracellular histone-induced FOXO4 expression. Targeting AMPK/FOXO4 might be a potential method for treating histone-mediated organ injury.

RESULTS

Extracellular histones facilitate VSMC senescence and inflammation

A previous study reported that extracellular histones induce apoptosis of human endothelial cells [13]. However, the damage caused by extracellular histones in VSMCs remains unclear. In this study, VSMCs were treated with various concentrations of extracellular histones, and cell viability was examined using flow cytometry. As shown in Figure 1A, cell viability was hardly reduced at 25 μg/mL; however, the reduction in the number of cells was more pronounced when the cells were incubated with 50–100 μg/mL histones. However, the number of cells incubated with 150 μg/mL histones did not change significantly compared with that incubated with 100 μg/mL histones. After 6 h of treatment with 100 μg/mL histones, the number of cells began to significantly reduce, which was not significantly different from that at 12 and 24 h (Figure 1B). To examine whether histones facilitate VSMC senescence, we performed SA β-gal staining. The results showed that as the concentration of histones increased, the number of SA β-gal-positive cells also increased (Figure 1C and 1D). Western blotting analysis showed similar results through assessment of senescence marker genes (Figure 1E and 1F). Next, we investigated the expressions of inflammatory cytokines after VSMC treatment with varying concentrations of extracellular histones. As expected, histone treatment significantly increased the mRNA expressions of IL-β, TNF-α, and IL-18 in a dose-dependent manner (Figure 1G–1I). These data suggest a function of extracellular histones in VSMC senescence and inflammation in organ injury.

Extracellular histones promote inflammasome assembly

To explore how extracellular histones exert their functions, the expression of inflammasome molecules in VSMCs treated with various concentrations of histones were tested. As indicated in Figure 2A and 2B, histone treatment markedly elevated NLRP3, apoptosis associated speck-like protein containing CARD (ASC), and caspase-1 protein levels in VSMCs. RT-qPCR showed the same results (Figure 2C). Next, we performed double immunofluorescence staining and found that as the number of histones increased, ASC and NLRP3 expression increased and were co-located in the cytoplasm (Figure 2D and 2E). To investigate whether histones affect inflammasome assembly, co-immunoprecipitation (CoIP) assay was performed. The results indicated that histone treatment significantly increased the interaction of ASC and NLRP3 in VSMCs (Figure 2F). Collectively, these data support the role of histones in inflammasome assembly regulation.

FOXO4 is a downstream regulator of histone-treated VSMC

To investigate how histones regulate inflammation and senescence, we partly examined candidate genes

reported with abnormal expression in organ injury [21, 22]. As indicated in Figure 3A, histone treatment significantly increased FOXO4, NR1H4, and HOXA9 expression and reduced HMGB1 expression in VSMCs. Next, FOXO4 expression at different concentrations of histone cell treatment was confirmed. The results showed that the mRNA and protein levels of FOXO4 dose-dependently increased (Figure 3B–3D). Consistent with this, immunofluorescence staining indicated similar results (Figure 3E). Besides, p21 expression increased with FOXO4 in histone-treated VSMCs (Figure 3E and 3F). These data suggest that FOXO4 is a downstream effector molecule of histones and may participate in VSMC senescence.

FOXO4 is involved in the histone-induced VSMC inflammatory response and senescence

To study the function of FOXO4 in VSMCs, FOXO4 was knocked down with two shRNAs and effect of the knockdown was confirmed. As indicated in Figure 4A–4C, transfection of shFOXO4-1# or shFOXO4-2# significantly reduced mRNA and protein levels. Next, FOXO4 was knocked down and then treated with

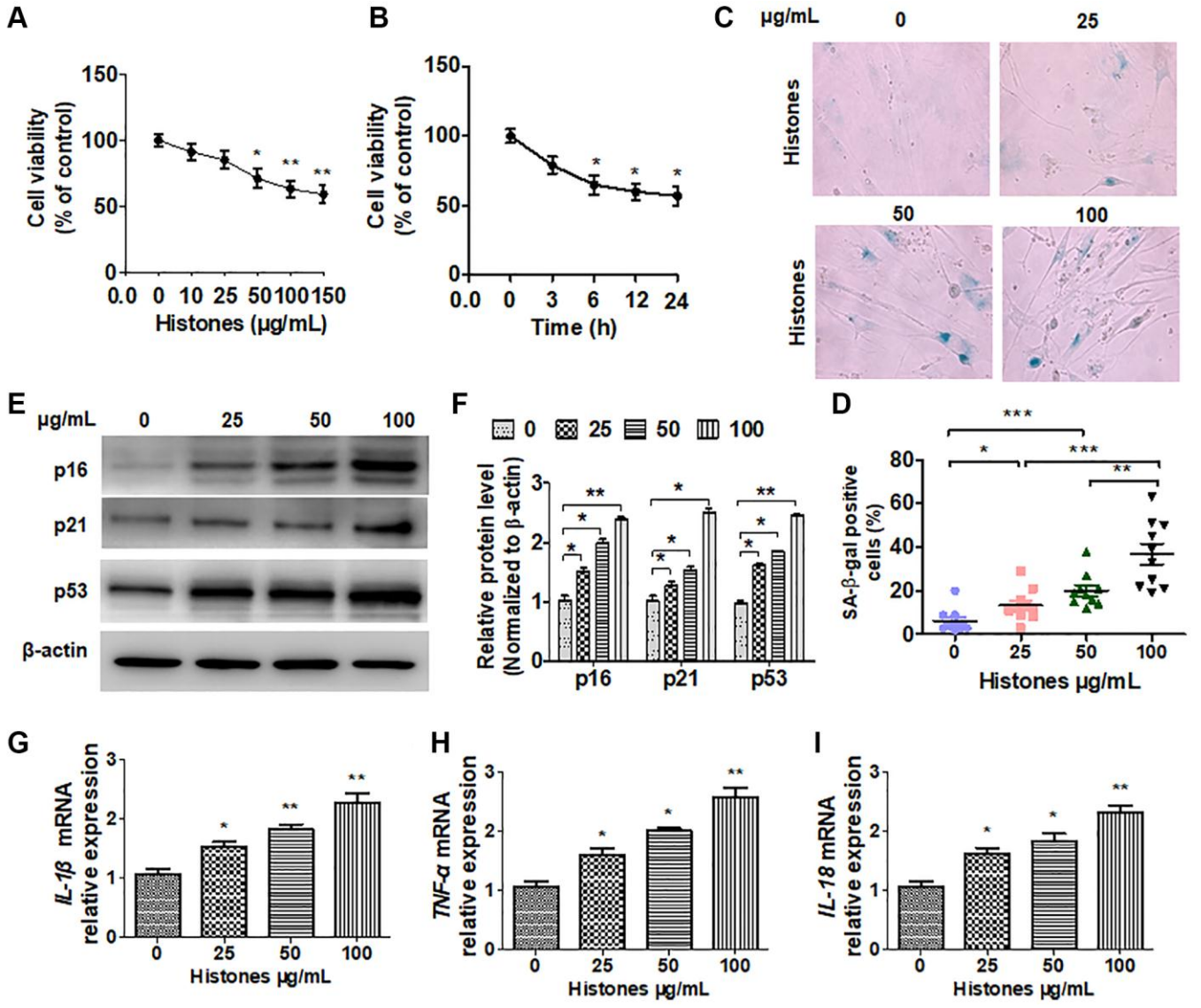

Figure 1. Extracellular histones promote VSMC senescence and the inflammatory response. VSMCs were treated with various concentrations of histones (0, 10, 25, 50, 100 and 150 μg/mL). (**A**) The CCK-8 assay was performed to determine cell viability. (**B**) Cells were treated with 100 μg/mL histones, and the CCK-8 assay was performed to determine cell viability at different time points. (**C**) SA β-gal staining was used to evaluate cell senescence. (**D**) Quantitative analysis of SA β-gal-positive VSMCs. (**E**) Western blotting was performed to analyze p16, p21, and p53 protein expression. (**F**) Quantitative analysis of (**E**). (**G–I**) RT-qPCR was performed to determine the expressions of inflammatory cytokines IL-β, TNF-α, and IL-18. For (**A**, **B**, **D**, and **F–I**), data are from three independent experiments; mean ± SEM; Student's *t*-test, $^{*}P < 0.05$, $^{**}P < 0.01$, and $^{***}P < 0.001$ vs. the corresponding control.

histones in VSMCs. We found that histone treatment markedly promoted an SA β-gal-positive cell number, while FOXO4 depletion simultaneously reversed these effects (Figure 4D and 4E). In parallel, FOXO4 deletion significantly suppressed the histone-induced promotion of inflammatory cytokine expression in VSMCs (Figure 4F and 4G). Collectively, these data establish that FOXO4 regulates histone-induced VSMC inflammatory response and senescence.

The AMPK signaling pathway mediates extracellular histone-upregulated FOXO4 expression

To identify which signaling pathway may regulate FOXO4 expression by extracellular histones, VSMCs were treated with and without histones. Western blotting was used to examine the molecular expression of the signal pathway. The results indicated that histones decreased the protein levels of p-AKT, p-Rb1,

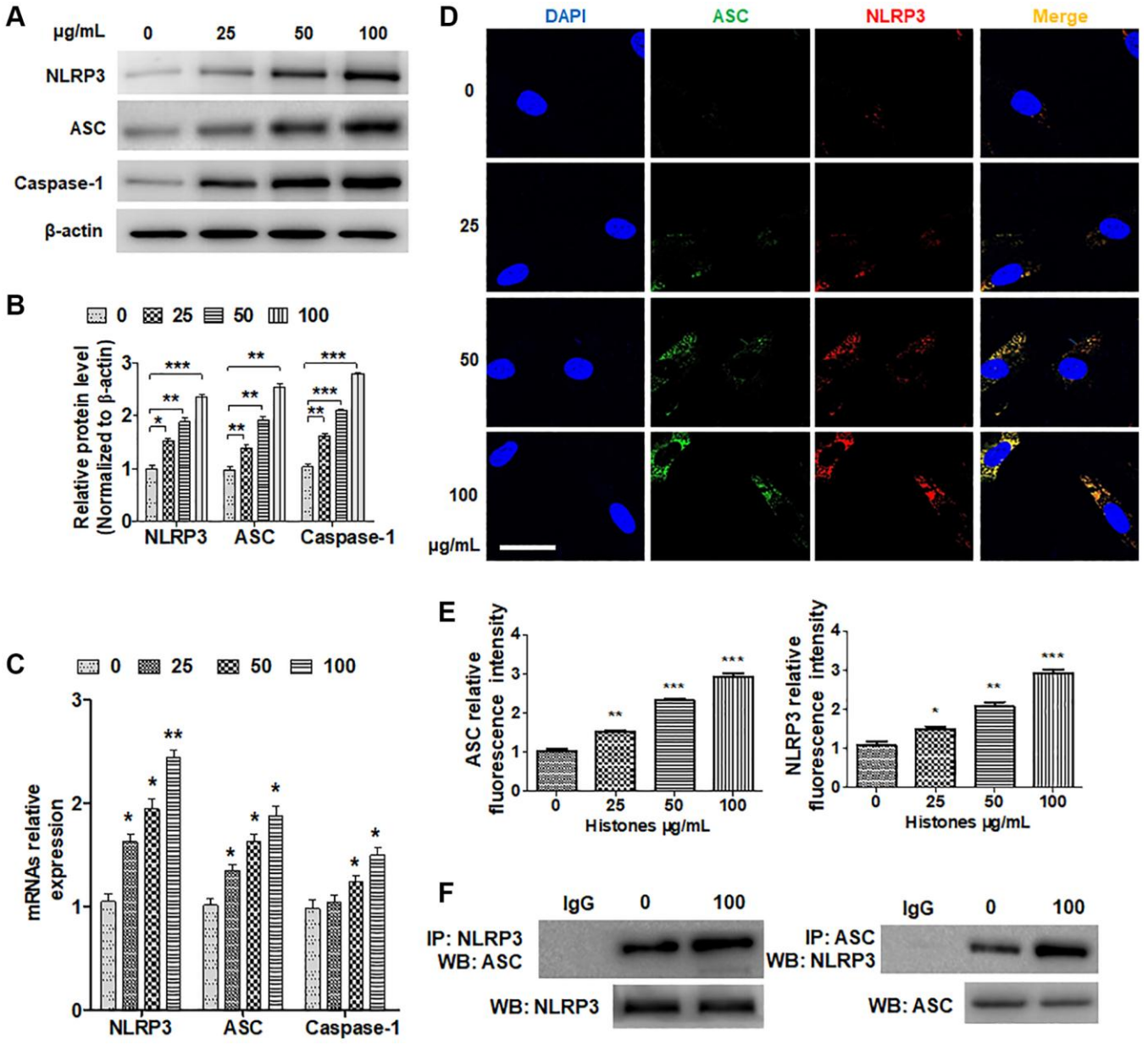

Figure 2. Extracellular histones facilitate NLRP3 inflammasome assembly. VSMCs were treated with various concentrations of histones (0, 10, 25, 50, and 100 μg/mL) for 6 h. (**A**) Western blotting was performed to analyze NLRP3, ASC, and caspase-1 inflammasome protein expression. (**B**) Quantitative analysis of (**A**). (**C**) RT-qPCR was performed to determine the mRNA expressions of NLRP3, ASC, and caspase-1. (**D**) Double immunofluorescence staining was performed to explore ASC and NLRP3 expression and colocation (green, ASC; red, NLRP3; blue, DAPI). Bar = 25 μm. (**E**) Quantitative analysis of the fluorescence intensity of ASC and NLRP3 from (**D**). (**F**) VSMCs were treated with or without histones (100 μg/mL), and CoIP was performed to examine the interaction of NLRP3 and ASC. For (**B**, **C** and **E**), data are from three independent experiments; mean ± SEM; Student's *t*-test, $^{*}P < 0.05$, $^{**}P < 0.01$, and $^{***}P < 0.001$ vs. the corresponding control.

and p-mTOR but increased AMPK and p-AMPK expression (Figure 5A and 5B). A previous study reported that Rb-1 was an upstream inhibitor of FOXO4 [23]. Next, an AKT (LY294002) and AMPK (BML-275) inhibitor was used to stimulate histone-treated VSMCs and confirmed that BML-275 could inhibit histone-promoted NLRP3, p21, and FOXO4 expression and increase histone-suppressed p-Rb1 expression (Figure 5C and 5D). Furthermore, the expression of inflammatory cytokines in BML-275-treated VSMCs has been examined after shFOXO4 transfection. It was found that FOXO4 depletion significantly downregulated IL-β, and TNF-α expression in VSMCs, while simultaneous BML-275 treatment has further enhanced this effect (Figure 5E). Together, these data showed that the AMPK signal pathway is involved in histone-regulated FOXO4 expression and could be a vital regulator in histone-mediated organ injury.

Blocking the AMPK signal pathway inhibits vascular inflammation induced by extracellular histones *in vitro*

To examine the effect of extracellular histones on VSMCs *in vivo*, mice were treated with histones while

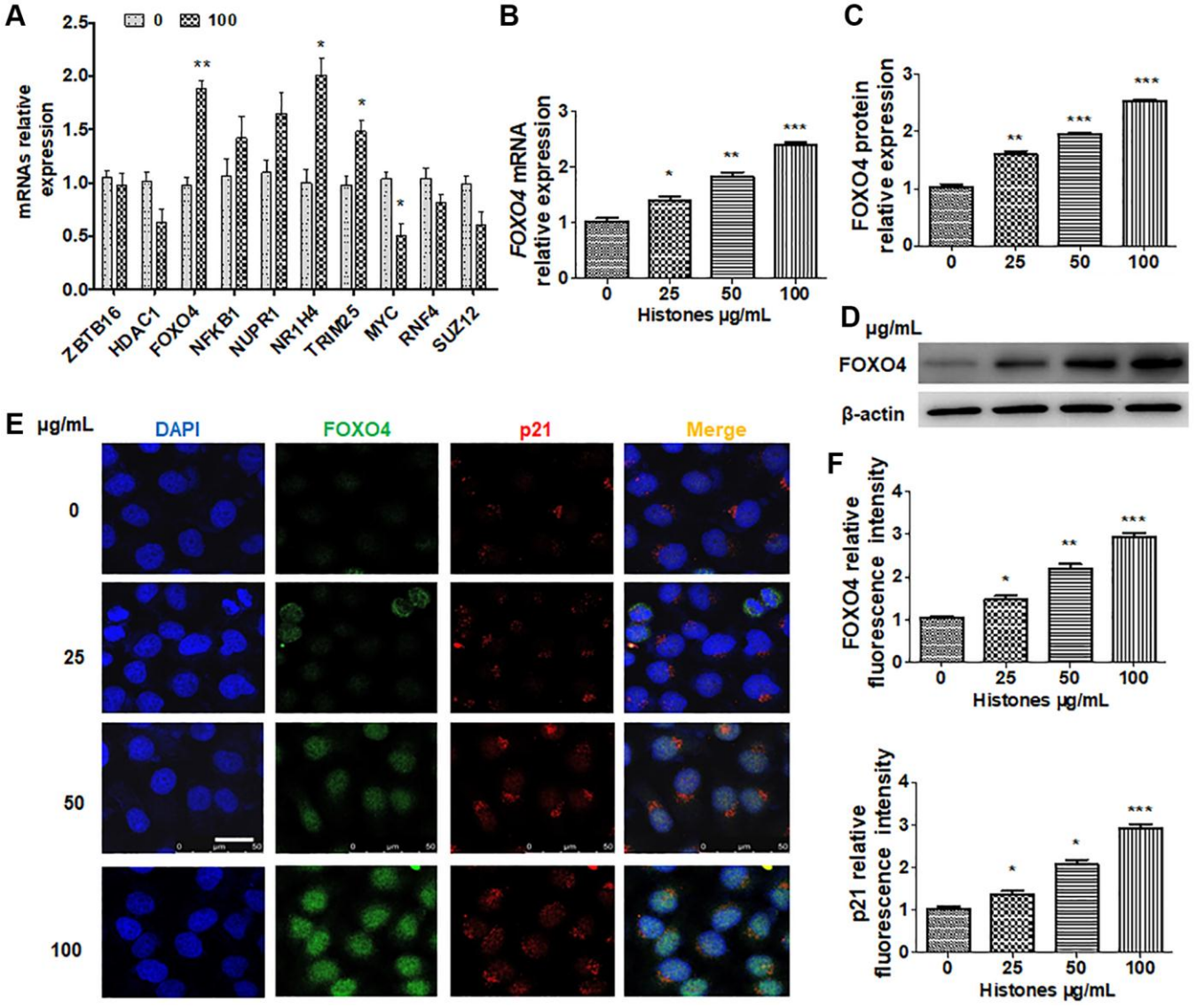

Figure 3. FOXO4 is a downstream target of histone-regulated senescence and inflammation in VSMCs. (**A**) VSMCs were treated with or without histones (100 μg/mL), and RT-qPCR was performed to determine candidate gene expression. (**B–D**) VSMCs were treated with various concentrations of histones, and FOXO4 mRNA expression was determined using RT-qPCR (**B**) or western blotting (**C** and **D**). (**E**) VSMCs were treated with various concentrations of histones, and double immunofluorescence staining was performed to determine FOXO4 and p21 expressions. (**F**) Quantitative analysis of the fluorescence intensity of FOXO4 and p21 from (**E**). For (**A**, **B**, **C**, and **F**), data are from three independent experiments; mean ± SEM; Student's *t*-test, $^{*}P < 0.05$, $^{**}P < 0.01$, and $^{***}P < 0.001$ vs. the corresponding control.

giving BML-275 treatment or not. The results showed that histone treatment markedly upregulated ACS and NLRP3 expression in the layer of VSMCs. However, the BML-275 treatment significantly reversed these

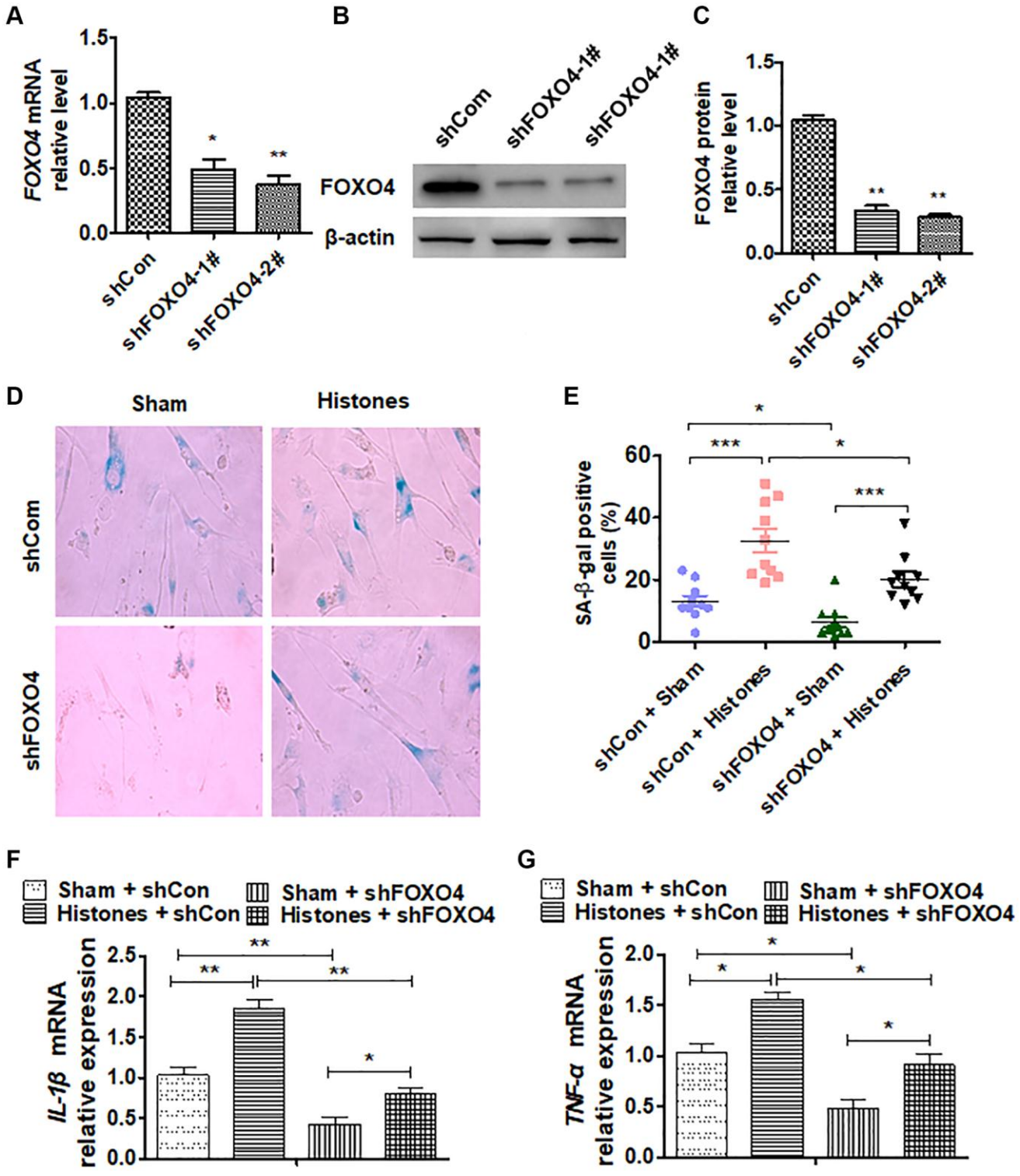

Figure 4. FOXO4 is involved in extracellular histone-facilitated VSMC inflammation and senescence. (**A**–**C**) VSMCs were transfected with shFOXO4-1#, shFOXO4-2#, or shCon vectors; then, RT-qPCR and western blot were performed to determine FOXO4 expression. (**D**) VSMCs were treated with histones after being transfected with shFOXO4 or shCon vector, and SA β-gal staining was performed to evaluate cell senescence. (**E**) Quantitative analysis of relative SA β-gal-positive cell numbers from (**D**). (**F** and **G**) RT-qPCR was performed to determine the expressions of the inflammatory cytokines IL-β and TNF-α in VSMCs after the indicated treatment. For (**A**, **C**, **E**, **F**, and **G**), data are from three independent experiments; mean ± SEM; Student's *t*-test, $^{*}P < 0.05$ and $^{**}P < 0.01$ vs. the corresponding control.

effects (Figure 6A and 6B). In parallel, extracellular histones increased the expression of the inflammatory cytokines IL-β, and TNF-α in VSMCs *in vitro*, while BML-275 treatment simultaneously depressed their expression (Figure 6C). To study whether BML-275 has a beneficial effect on decreasing histone-induced organ damage, the levels of cardiac troponin I (cTnI), alanine aminotransferase (ALT), and blood urea nitrogen (BUN) in the serum of mouse models were tested. As indicated in Supplementary Figure 1, histones-treated mice significantly increase ALT, BUN and cTnl levels in serum. However, BML-275 treatment markedly reduces these protein levels in histones-induced mice. Additionally, double immunofluorescence staining showed that extracellular histones elevated FOXO4 and p21 expression in VSMCs *in vitro*, but blocking the AMPK signal pathway with BML-275 reversed the expression of these genes (Figure 6D and 6E). Additionally, extracellular histones significantly promoted senescence relative marker gene *p16*, *p21*, and *p53* expression, while BML-275 treatment decreased this promotion of histones (Figure 6F). To examine whether histones or histones + BML-275 treatment *in vivo* affected the AMPK/FOXO4 pathway, we detected these proteins level by Western blotting. As indicated in Supplementary Figure 2, the expression of p-AMPK and FOXO4 was significantly elevated in histones-treated vascular tissue. However, p-AMPK and FOXO4 protein levels were depressed while BML-275 treatment simultaneously. Together, these results showed that extracellular histones significantly promote inflammation and senescence in VSMCs, and blocking the AMPK signaling pathway by BML-275 would partly reverse these effects.

DISCUSSION

In this study, we explored the role of extracellular histones in regulating the senescence and inflammation of VSMCs via the AMPK/FOXO4 axis. We found that

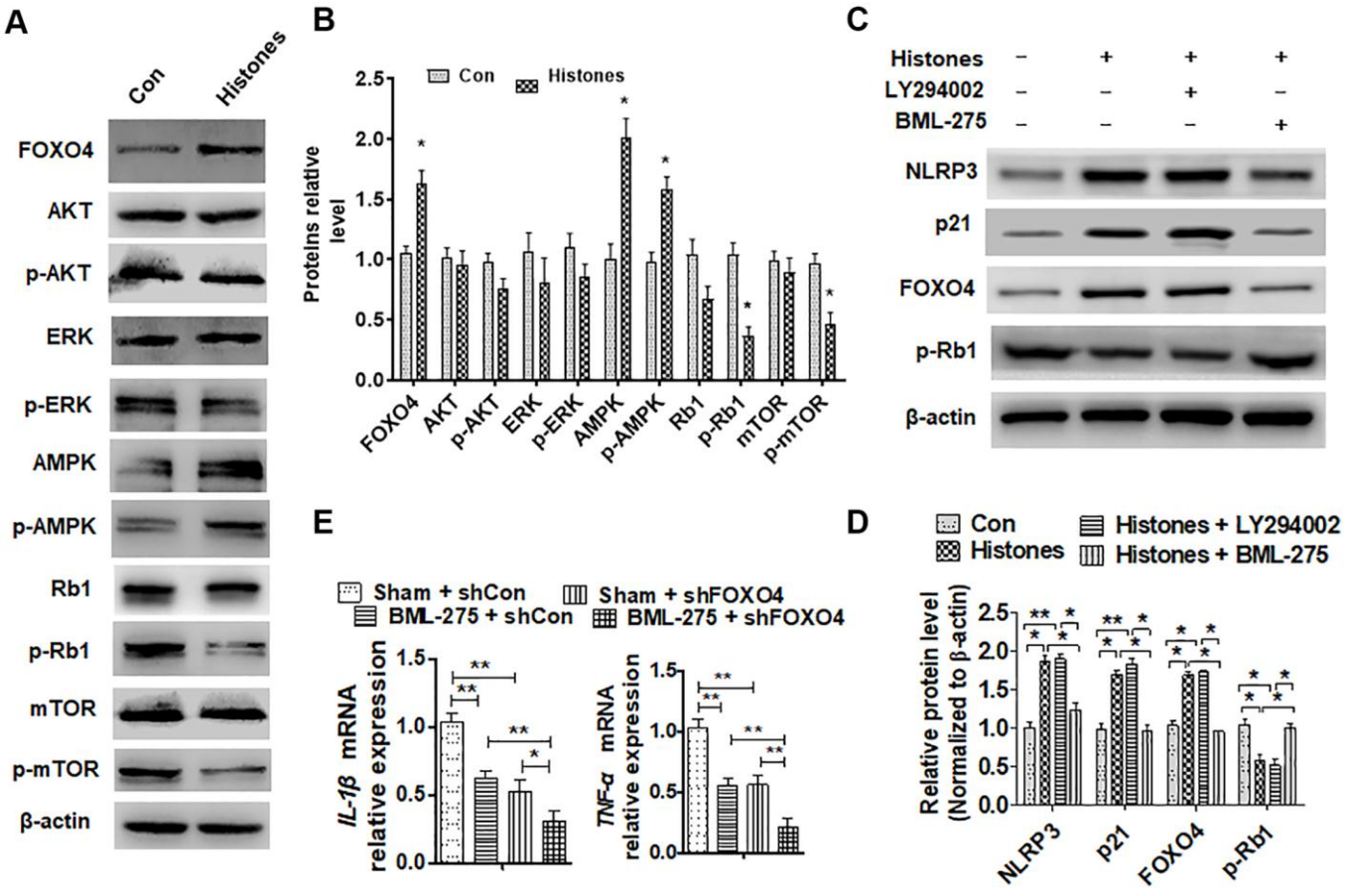

Figure 5. The AMPK signaling pathway mediates extracellular histone-upregulated FOXO4 expression. (**A**) VSMCs were treated with or without histones; then, western blot was used to examine the protein level of the signal pathway molecule. (**B**) Quantitative analysis of (**A**). (**C**) VSMCs were treated with histones and then incubated with the AKT pathway inhibitor (LY94002) or the AMPK pathway inhibitor (BML-275) for 6 h. NLRP3, p21, FOXO4, and p-Rb1 protein levels were determined using western blotting. (**D**) Quantitative analysis of (**C**). (**E**) IL-β and TNF-α expressions were determined using RT-qPCR in BML-275-treated VSMCs after shFOXO3 transfection. For (**B**, **E**, and **D**), data are from three independent experiments; mean ± SEM; Student's *t*-test, $^{*}P < 0.05$ and $^{**}P < 0.01$ vs. the corresponding control.

extracellular histones induced senescence and the inflammatory response of VSMCs in a dose-dependent manner. We also found that FOXO4, which is a downstream effector molecule of extracellular histones, is involved in histone-regulated VSMC inflammatory response and senescence. Furthermore, the AMPK signaling pathway was found to mediate extracellular histone-induced FOXO4 expression. Disruption of the AMPK signaling pathway by inhibitors obstructed extracellular histone-induced vascular inflammation *in vivo* and *in vitro* (Figure 7).

Endothelial cells play an important role in vascular dysfunction associated with sepsis [24, 25]. However, increasing evidence has demonstrated that VSMCs are involved in sepsis in a manner that is independent of endothelial cells [26, 27]. Because VSMCs are not in direct contact with the bloodstream, it appears that

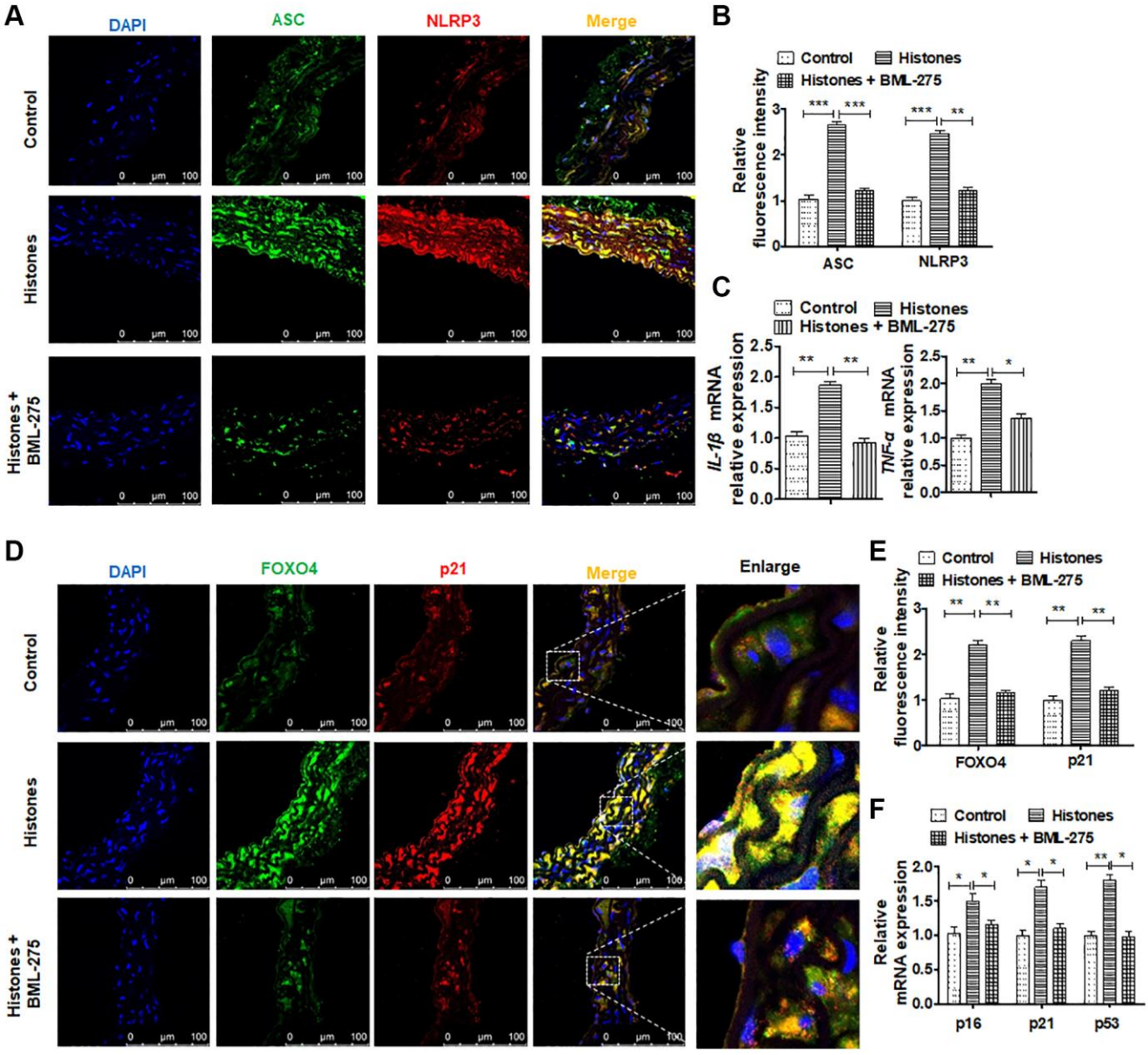

Figure 6. Blocking the AMPK signaling pathway can inhibit vascular inflammation induced by extracellular histones. (**A**) Mice were treated with saline (n = 18), histones (n = 18), or histones + BML-275 (n = 18) for 24 h. Double immunofluorescence staining was used to measure the expression of ASC and NLRP3 in the blood vessels (green, ASC; red, NLRP3; blue, DAPI). Bar = 100 μm. (**B**) Quantitative analysis of the fluorescence intensity of ASC and NLRP3 from (**A**). (**C**) RT-qPCR was performed to determine IL-β and TNF-α expressions in the mice treated as stated above. (**D**) Double immunofluorescence staining was performed to measure the expression of FOXO4 and p21 in the blood vessels (green, FOXO4; red, p21; blue, DAPI). Bar = 100 μm. (**E**) Quantitative analysis of the fluorescence intensity of FOXO4 and p21 from (**A**). (**F**) RT-qPCR was performed to determine p16, p21, and p53 expressions in the mice treated as stated above. For (**B**, **D**, **E** and **F**), data are from three independent experiments; mean ± SEM; Student's t-test, $^{*}P < 0.05$, $^{**}P < 0.01$, and $^{***}P < 0.001$ vs. the corresponding control.

sepsis damages VSMCs after the improvement of acute illness. In the early and late stages of sepsis, the contractile function of VSMCs is impaired [28]. This shows that VSMCs might be involved in the entire sepsis process. Macrophages treated with LPS release a large number of extracellular histones that interact with target cell receptors (especially TLR4) to promote inflammation [29]. In sepsis, alterations in the normal autoregulation of perfusion and the toxic effects of the media can lead to severe organ dysfunction [7]. Although VSMCs have been shown to play a key role in sepsis [19, 20], the effect of extracellular histones on VSMCs in sepsis is unclear. In this study, we found that extracellular histones induced the senescence and inflammatory response of VSMCs in a dose-dependent manner. FOXO4 is involved in histone-regulated VSMC inflammatory response and senescence. Blocking of the AMPK signaling pathway by inhibitors altered extracellular histones-induced vascular inflammation. We found that histones significantly activated the inflammatory response of VSMCs. Previous studies reported that extracellular histones target TLR2, 4, and 9 in various cell types and activate cellular inflammation and cell damage [30–32]. For example, histones cause glomerular cell damage by activating TLR2 and 4 [33] and hepatic reperfusion injury by activating TLR9 [34]. TLRs are a vital inflammatory response pathway. Additionally, several studies have indicated that TLRs are closely related to AMPK signaling pathways [35–38]. Therefore, we speculated that TLRs are potential receptors for histones and activate the AMPK signaling pathway.

The FOXO family of proteins comprise a series of transcription factors, including FOXO1, FOXO3a, FOXO4, and FOXO6 [39]. According to upstream and downstream gene regulation, FOXO4 can be used as a transcriptional activator and repressor [40, 41]. Several studies have shown that FOXO4 is involved in the regulation of various processes, including cell proliferation, apoptosis, autophagy, cell senescence, inflammation, and energy production [42–46]. Zhang *et al*. found that GUARDIN serves as a scaffold to stabilize the LRP130/PGC1α heterodimer to promote FOXO4 expression and upregulate the expression of the target gene *p21*, causing cell senescence [47]. The activation of FOXO4 in melanoma promotes the transcription of *p21* and subsequently accelerates cell senescence [48]. Using FOXO4-knockout mice, Zhu *et al*. found that FoxO4 promotes early inflammatory response in myocardial infarction by regulating Arg1 expression [45]. Blocking the interaction between XBP1u and FoxO4 promoted the nuclear translocation of FoxO4, promoted *in vitro* proinflammatory activity, and stimulated the formation of aortic aneurysms [49]. In the present study, extracellular histones promoted FOXO4 expression, which is then involved in the histone-regulated VSMC inflammatory response and senescence. Deletion of FOXO4 suppressed the promoting effect of histones on inflammatory cytokine expression and SA β-gal-positive cells in VSMCs.

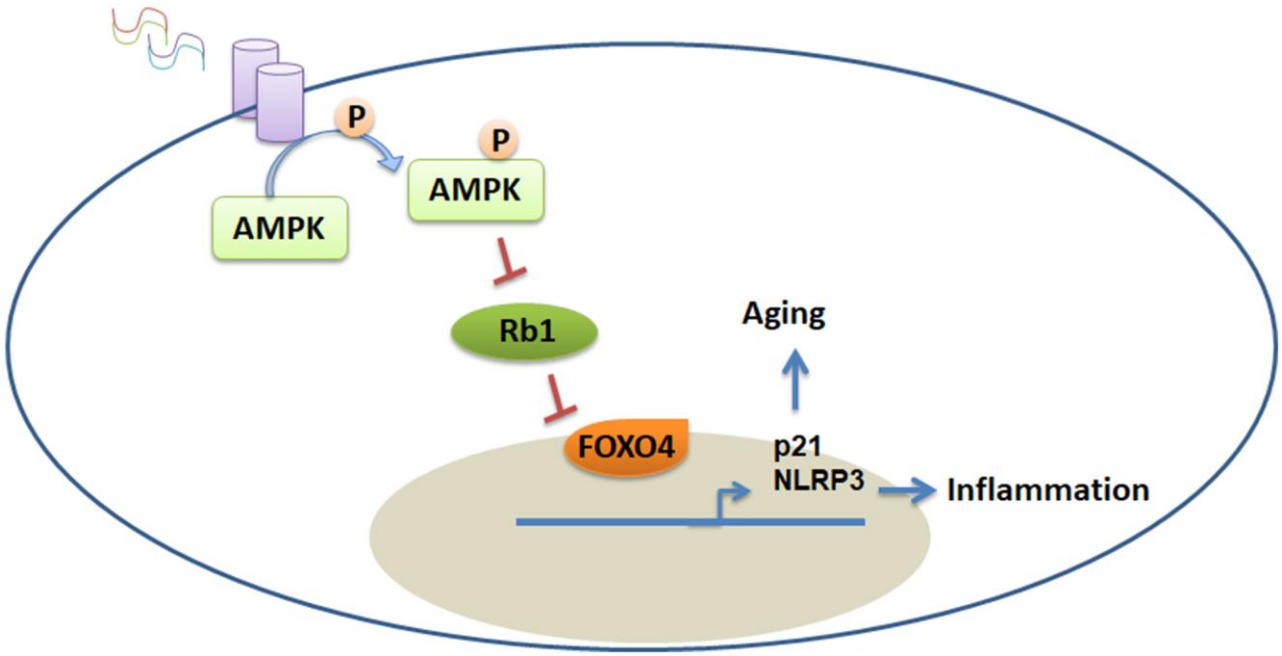

Figure 7. Proposed model for extracellular histone-mediated inflammation and senescence in VSMCs. Extracellular histones activate the AMPK pathway, which then promotes FOXO4 phosphorylation and entry into the nucleus. FOXO4 subsequently promotes p21 and NLRP3 expression.

In conclusion, extracellular histones damaged VSMCs *in vivo* and *in vitro*. Extracellular histones induced an inflammatory response and senescence of VSMCs. FOXO4 expression was mediated by the AMPK signaling pathway in histone-treated VSMCs. Deleting FOXO4 or blocking the AMPK signaling pathway could relieve the extracellular histone-induced inflammatory response and senescence of VSMCs. AMPK/FOXO4 might be potential targets in the treatment of histone-mediated organ injury.

MATERIALS AND METHODS

Cell culture and treatment

Mouse aortic vascular smooth muscle cells (ATCC, No.CRL-2797TM) were routinely cultured in low-glucose Dulbecco's modified Eagle's medium (Gibco Life Technologies, Rockville, MD) containing 100 units/ml of penicillin, 100 μg/ml of streptomycin, and 10% fetal bovine serum (Gibco) in a humidified incubator at 37°C with 5% CO_2. The cells from passages 3 to 6 were used in all studies. The cells were maintained in 5% CO_2 at 37°C within a humidified atmosphere, and their morphology and α-SMA expression were evaluated. When the cells attained 80% confluence, the media was replaced, and the cells were exposed for 6 h to various concentrations of calf thymus histone (10, 25, 50, or 100 μg/mL prepared in PBS; pH 7.4 [Gibco]) [50]. LY294002 (Selleck) was used as a PI3K/AKT inhibitor, as previously described [51]. The AMPK inhibitor BML-275 (4 μM; Selleck) was used in this study [52].

Western blotting

According to a previous description [4], radioimmunoprecipitation assay lysis buffer was used to extract proteins from cultured VSMCs. The proteins were then separated using 8% or 10% SDS-PAGE and electrotransferred to PVDF membrane (Millipore). After blocking in 5% milk in TBS for 2 h, the membrane was incubated overnight at 4°C with the primary antibody. The signal was detected using ECL (enhanced chemiluminescence) Fuazon Fx (Vilber Lourmat). The following antibodies were used: anti-p16 (1:1000), anti-p21 (1:1000), anti-p53 (1:1000), anti-NLRP3 (1:1000), anti-ASC (1:500), anti-caspase-1 (1:1000), anti-FOXO4 (1:1000), anti-AKT (1:500), anti-p-AKT (1:1000), anti-ERK (1:1000), anti-p-ERK (1:1000), anti-AMPK (1:1000), anti-p-AMPK (1:1000), anti-Rb1 (1:1000), anti-p-Rb1 (1:1000), anti-mTOR (1:1000), anti-p-mTOR (1:1000), and anti-β-actin (1:1000). The images were captured and processed using FusionCapt Advance Fx5 software (Vilber Lourmat). All experiments were conducted in triplicate independently.

RNA extraction and RT-qPCR

The VSMCs were lysed, and total RNA was extracted according to the instructions of the E.Z.N.A.®Total RNA Kit I (R6834-01) manual. A NanoDrop 2000 (Thermo Fisher) spectrophotometer was used to determine the concentration and purity of the RNA. Reverse RNA transcription was then performed using the M-MLV first-strand kit (Life Technologies) for mRNA expression analysis. Then, the Platinum SYBR Green qPCR SuperMix-UDG kit (Invitrogen) was used for mRNA RT-qPCR. RT-qPCR was performed on a CFX96™ real-time system (Bio-Rad). The primers used are listed in Supplementary Table 1. The $2^{-\Delta\Delta Ct}$ method was used to normalize the gene expression of GAPDH.

SA β-gal staining and quantitative analysis

The cells were stained with SA β-gal to detect cell senescence, as previously described [53]. Briefly, VSMCs were seeded on a 12-well plate and incubated at 37°C with 5% CO_2 for 48 h. Then, the cells were fixed for 15 min, washed with PBS, and incubated with the staining mixture at 37°C for 18 h. The staining mixture of the SA-β-gal staining kit (Abcam, Inc.) was used. Quantification of the SA β-gal-stained cells was performed using Image-Pro Plus 6.0 (Media Cybernetics, Rockville, MD, USA).

Immunofluorescence staining

The cells were placed on a slide, fixed with 4% formaldehyde for 15 min, and washed with PBS. The slide was incubated with 10% normal goat serum (710 027, KPL) at room temperature for 30 min and later incubated overnight with the corresponding primary antibody at 4°C. After washing with PBS, the slide was incubated for 2 h with a fluorescent-labeled IgG antibody (021815 or 031506, KPL, SeraCare Life Sciences, Inc., USA). Finally, the cell smear was treated with DAPI for 15 min for nuclear counterstaining. The images were acquired using a confocal microscope (DM6000CFS, Leica) and digitized using LAS AF software.

CoIP assay

CoIP was performed as previously described [4]. In brief, the cell lysates were immunoprecipitated with the indicated antibody at 4°C overnight and then incubated with protein A-agarose at 4°C for 1 h. Protein A-agarose–antigen–antibody complexes were then collected by centrifugation at 12,000 g for 2 min at 4°C and washed five times with 1 ml immunoprecipitation-HAT buffer for 20 min at 4°C.

The bound proteins were resolved using SDS-PAGE, followed by western blotting with the corresponding antibody.

Animal experiments

Male C57BL/6 mice (12–16-week old) were reared under a 12-h light cycle with drinking water and a standard laboratory diet provided ad libitum [4]. The mice were anesthetized with isoflurane (2.5%); a single intravenous injection of histone 45 mg/kg (consisting of 7.5% H1, 20.8% H2A, 32.5% H2B, 10.2% H3, and 28.9% H4) [18] and BML-275 (0.5 mg/kg) + histone 45 mg/Kg intravenously. We injected 0.05 mg/kg/ buprenorphine for pain control and saline (50 ml/kg) for liquid supply subcutaneously at 1 and 12 h, and blood samples were collected from the tail veins before and 8 h after injection. The mice were euthanized 24 h after the histone or saline injection, and blood vessels and other tissues were collected and stored. All procedures were performed in accordance with the Research Ethics Committee of Guangdong Provincial People's Hospital (No.KY-D-2021-018-01).

Cell counting Kit-8 assay

VSMCs were seeded in 96-well plates (2×10^4 cells/well) and cultured for 24 h, as previously described [4]. Then, 5, 10, 20, and 40 μM MC were added to the media for 24 h. The viability of VSMCs was determined using Cell Counting Kit-8 (CCK-8) assays. After culture, 10 μl of CCK-8 reagent (Beibo, China) was added to each well, and the plates were incubated at 37°C in a humidified atmosphere containing 5% CO_2 for 2.5 h. The absorbance was read at 450 nm on a microplate reader (Thermo Fisher Scientific).

Statistical analysis

All data are presented as means ± standard error of the mean. Between-group differences were analyzed using Student's *t*-test. Analysis of variance was performed for statistical analysis of multiple groups. Spearman's correlation was used to determine the correlation between two genes. *P*-values of <0.05 were considered statistically significant.

Abbreviations

ASC: apoptosis associated speck-like protein containing CARD; NLRP3: NACHT, LRR and PYD domains-containing protein 3; FOXO4: forkhead box protein O4; LPS: lipopolysaccharide; AMPK: 5′-AMP-activated protein kinase; VSMC: vascular smooth muscle cell.

AUTHOR CONTRIBUTIONS

Hang Yang and Yong-Yan Luo conceived and designed the experiments. Hang Yang, Kai-Ran He, and Lue-Tao Zhang performed all the experiments. Kai-Ran He and Hang Yang analyzed the data. Xiao-Jun Lin and Yang Hang wrote the manuscript. All authors read and approved the final manuscript.

CONFLICTS OF INTEREST

The authors declare no conflicts of interest related to this study.

FUNDING

This work was supported by Zhuhai Medical Research Fund Project (no. 911292645025).

REFERENCES

1. Gotts JE, Matthay MA. Sepsis: pathophysiology and clinical management. BMJ. 2016; 353:i1585. https://doi.org/10.1136/bmj.i1585 PMID:27217054

2. Fleischmann C, Scherag A, Adhikari NK, Hartog CS, Tsaganos T, Schlattmann P, Angus DC, Reinhart K, and International Forum of Acute Care Trialists. Assessment of Global Incidence and Mortality of Hospital-treated Sepsis. Current Estimates and Limitations. Am J Respir Crit Care Med. 2016; 193:259–72. https://doi.org/10.1164/rccm.201504-0781OC PMID:26414292

3. Xie J, Wang H, Kang Y, Zhou L, Liu Z, Qin B, Ma X, Cao X, Chen D, Lu W, Yao C, Yu K, Yao X, et al, and Chinese Epidemiological Study of Sepsis (CHESS) Study Investigators. The Epidemiology of Sepsis in Chinese ICUs: A National Cross-Sectional Survey. Crit Care Med. 2020; 48:e209–18. https://doi.org/10.1097/CCM.0000000000004155 PMID:31804299

4. Zheng C, Li D, Zhan W, He K, Yang H. Downregulation of SENP1 suppresses LPS-induced macrophage inflammation by elevating Sp3 SUMOylation and disturbing Sp3-NF-κB interaction. Am J Transl Res. 2020; 12:7439–48. PMID:33312380

5. Gyawali B, Ramakrishna K, Dhamoon AS. Sepsis: The evolution in definition, pathophysiology, and management. SAGE Open Med. 2019; 7:2050312119835043. https://doi.org/10.1177/2050312119835043 PMID:30915218

6. Touyz RM, Alves-Lopes R, Rios FJ, Camargo LL, Anagnostopoulou A, Arner A, Montezano AC. Vascular smooth muscle contraction in hypertension. Cardiovasc Res. 2018; 114:529–39. https://doi.org/10.1093/cvr/cvy023 PMID:29394331

7. Hollenberg SM, Cunnion RE. Endothelial and vascular smooth muscle function in sepsis. J Crit Care. 1994; 9:262–80. https://doi.org/10.1016/0883-9441(94)90006-x PMID:7889136

8. Rho SS, Ando K, Fukuhara S. Dynamic Regulation of Vascular Permeability by Vascular Endothelial Cadherin-Mediated Endothelial Cell-Cell Junctions. J Nippon Med Sch. 2017; 84:148–59. https://doi.org/10.1272/jnms.84.148 PMID:28978894

9. Lelubre C, Vincent JL. Mechanisms and treatment of organ failure in sepsis. Nat Rev Nephrol. 2018; 14:417–27. https://doi.org/10.1038/s41581-018-0005-7 PMID:29691495

10. Szatmary P, Huang W, Criddle D, Tepikin A, Sutton R. Biology, role and therapeutic potential of circulating histones in acute inflammatory disorders. J Cell Mol Med. 2018; 22:4617–29. https://doi.org/10.1111/jcmm.13797 PMID:30085397

11. Allam R, Kumar SV, Darisipudi MN, Anders HJ. Extracellular histones in tissue injury and inflammation. J Mol Med (Berl). 2014; 92:465–72. https://doi.org/10.1007/s00109-014-1148-z PMID:24706102

12. Abrams ST, Zhang N, Manson J, Liu T, Dart C, Baluwa F, Wang SS, Brohi K, Kipar A, Yu W, Wang G, Toh CH. Circulating histones are mediators of trauma-associated lung injury. Am J Respir Crit Care Med. 2013; 187:160–9. https://doi.org/10.1164/rccm.201206-1037OC PMID:23220920

13. Ibañez-Cabellos JS, Aguado C, Pérez-Cremades D, García-Giménez JL, Bueno-Betí C, García-López EM, Romá-Mateo C, Novella S, Hermenegildo C, Pallardó FV. Extracellular histones activate autophagy and apoptosis via mTOR signaling in human endothelial cells. Biochim Biophys Acta Mol Basis Dis. 2018; 1864:3234–46. https://doi.org/10.1016/j.bbadis.2018.07.010 PMID:30006152

14. Li Y, Wan D, Luo X, Song T, Wang Y, Yu Q, Jiang L, Liao R, Zhao W, Su B. Circulating Histones in Sepsis: Potential Outcome Predictors and Therapeutic Targets. Front Immunol. 2021; 12:650184. https://doi.org/10.3389/fimmu.2021.650184 PMID:33868288

15. Zetoune FS, Ward PA. Role of Complement and Histones in Sepsis. Front Med (Lausanne). 2020; 7:616957. https://doi.org/10.3389/fmed.2020.616957 PMID:33425963

16. Xu J, Zhang X, Pelayo R, Monestier M, Ammollo CT, Semeraro F, Taylor FB, Esmon NL, Lupu F, Esmon CT. Extracellular histones are major mediators of death in sepsis. Nat Med. 2009; 15:1318–21. https://doi.org/10.1038/nm.2053 PMID:19855397

17. Shi CX, Wang Y, Chen Q, Jiao FZ, Pei MH, Gong ZJ. Extracellular Histone H3 Induces Pyroptosis During Sepsis and May Act Through NOD2 and VSIG4/NLRP3 Pathways. Front Cell Infect Microbiol. 2020; 10:196. https://doi.org/10.3389/fcimb.2020.00196 PMID:32432055

18. Villalba N, Baby S, Cha BJ, Yuan SY. Site-specific opening of the blood-brain barrier by extracellular histones. J Neuroinflammation. 2020; 17:281. https://doi.org/10.1186/s12974-020-01950-x PMID:32962721

19. Strela FB, Brun BF, Berger RCM, Melo S, de Oliveira EM, Barauna VG, Vassallo PF. Lipopolysaccharide exposure modulates the contractile and migratory phenotypes of vascular smooth muscle cells. Life Sci. 2020; 241:117098. https://doi.org/10.1016/j.lfs.2019.117098 PMID:31794773

20. Zhao G, Zhong Y, Su W, Liu S, Song X, Hou T, Mu X, Gong MC, Guo Z. Transcriptional Suppression of CPI-17 Gene Expression in Vascular Smooth Muscle Cells by Tumor Necrosis Factor, Krüppel-Like Factor 4, and Sp1 Is Associated with Lipopolysaccharide-Induced Vascular Hypocontractility, Hypotension, and Mortality. Mol Cell Biol. 2019; 39:e00070–19. https://doi.org/10.1128/MCB.00070-19 PMID:30936247

21. Zhai J, Qi A, Zhang Y, Jiao L, Liu Y, Shou S. Bioinformatics Analysis for Multiple Gene Expression Profiles in Sepsis. Med Sci Monit. 2020; 26:e920818. https://doi.org/10.12659/MSM.920818 PMID:32280132

22. Balamuth F, Alpern ER, Kan M, Shumyatcher M, Hayes K, Lautenbach E, Himes BE. Gene Expression Profiles in Children With Suspected Sepsis. Ann Emerg Med. 2020; 75:744–54. https://doi.org/10.1016/j.annemergmed.2019.09.020 PMID:31983492

23. Endo M, Tanaka Y, Otsuka M, Minami Y. E2F1-Ror2 signaling mediates coordinated transcriptional

regulation to promote G1/S phase transition in bFGF-stimulated NIH/3T3 fibroblasts. FASEB J. 2020; 34:3413–28.
https://doi.org/10.1096/fj.201902849R
PMID:31922321

24. Joffre J, Hellman J, Ince C, Ait-Oufella H. Endothelial Responses in Sepsis. Am J Respir Crit Care Med. 2020; 202:361–70.
https://doi.org/10.1164/rccm.201910-1911TR
PMID:32101446

25. Zhou Y, Li P, Goodwin AJ, Cook JA, Halushka PV, Chang E, Fan H. Exosomes from Endothelial Progenitor Cells Improve the Outcome of a Murine Model of Sepsis. Mol Ther. 2018; 26:1375–84.
https://doi.org/10.1016/j.ymthe.2018.02.020
PMID:29599080

26. Englert JA, Christman JW, Ballinger MN. Unhinging the machinery of sepsis: An unexpected role for vascular smooth muscle. J Leukoc Biol. 2018; 104:661–3.
https://doi.org/10.1002/JLB.CE0618-236R
PMID:30134503

27. Sandbo N, Taurin S, Yau DM, Kregel S, Mitchell R, Dulin NO. Downregulation of smooth muscle alpha-actin expression by bacterial lipopolysaccharide. Cardiovasc Res. 2007; 74:262–9.
https://doi.org/10.1016/j.cardiores.2007.01.011
PMID:17303098

28. Wurster SH, Wang P, Dean RE, Chaudry IH. Vascular smooth muscle contractile function is impaired during early and late stages of sepsis. J Surg Res. 1994; 56:556–61.
https://doi.org/10.1006/jsre.1994.1089
PMID:8015311

29. Nair RR, Mazza D, Brambilla F, Gorzanelli A, Agresti A, Bianchi ME. LPS-Challenged Macrophages Release Microvesicles Coated With Histones. Front Immunol. 2018; 9:1463.
https://doi.org/10.3389/fimmu.2018.01463
PMID:29997623

30. Marsman G, Zeerleder S, Luken BM. Extracellular histones, cell-free DNA, or nucleosomes: differences in immunostimulation. Cell Death Dis. 2016; 7:e2518.
https://doi.org/10.1038/cddis.2016.410
PMID:27929534

31. Chen R, Xie Y, Zhong X, Fu Y, Huang Y, Zhen Y, Pan P, Wang H, Bartlett DL, Billiar TR, Lotze MT, Zeh HJ 3rd, Fan XG, et al. Novel chemokine-like activities of histones in tumor metastasis. Oncotarget. 2016; 7:61728–40.
https://doi.org/10.18632/oncotarget.11226
PMID:27623211

32. Xu J, Zhang X, Monestier M, Esmon NL, Esmon CT. Extracellular histones are mediators of death through TLR2 and TLR4 in mouse fatal liver injury. J Immunol. 2011; 187:2626–31.
https://doi.org/10.4049/jimmunol.1003930
PMID:21784973

33. Kumar SV, Kulkarni OP, Mulay SR, Darisipudi MN, Romoli S, Thomasova D, Scherbaum CR, Hohenstein B, Hugo C, Müller S, Liapis H, Anders HJ. Neutrophil Extracellular Trap-Related Extracellular Histones Cause Vascular Necrosis in Severe GN. J Am Soc Nephrol. 2015; 26:2399–413.
https://doi.org/10.1681/ASN.2014070673
PMID:25644111

34. Huang H, Evankovich J, Yan W, Nace G, Zhang L, Ross M, Liao X, Billiar T, Xu J, Esmon CT, Tsung A. Endogenous histones function as alarmins in sterile inflammatory liver injury through Toll-like receptor 9 in mice. Hepatology. 2011; 54:999–1008.
https://doi.org/10.1002/hep.24501
PMID:21721026

35. Deng JS, Jiang WP, Chen CC, Lee LY, Li PY, Huang WC, Liao JC, Chen HY, Huang SS, Huang GJ. *Cordyceps cicadae* Mycelia Ameliorate Cisplatin-Induced Acute Kidney Injury by Suppressing the TLR4/NF-κB/MAPK and Activating the HO-1/Nrf2 and Sirt-1/AMPK Pathways in Mice. Oxid Med Cell Longev. 2020; 2020:7912763.
https://doi.org/10.1155/2020/7912763
PMID:32089779

36. Liu Y, Nguyen PT, Wang X, Zhao Y, Meacham CE, Zou Z, Bordieanu B, Johanns M, Vertommen D, Wijshake T, May H, Xiao G, Shoji-Kawata S, et al. TLR9 and beclin 1 crosstalk regulates muscle AMPK activation in exercise. Nature. 2020; 578:605–9.
https://doi.org/10.1038/s41586-020-1992-7
PMID:32051584

37. Vaez H, Najafi M, Toutounchi NS, Barar J, Barzegari A, Garjani A. Metformin Alleviates Lipopolysaccharide-induced Acute Lung Injury through Suppressing Toll-like Receptor 4 Signaling. Iran J Allergy Asthma Immunol. 2016; 15:498–507.
PMID:28129682

38. Tadie JM, Bae HB, Deshane JS, Bell CP, Lazarowski ER, Chaplin DD, Thannickal VJ, Abraham E, Zmijewski JW. Toll-like receptor 4 engagement inhibits adenosine 5'-monophosphate-activated protein kinase activation through a high mobility group box 1 protein-dependent mechanism. Mol Med. 2012; 18:659–68.
https://doi.org/10.2119/molmed.2011.00401
PMID:22396017

39. Tia N, Singh AK, Pandey P, Azad CS, Chaudhary P, Gambhir IS. Role of Forkhead Box O (FOXO) transcription factor in aging and diseases. Gene. 2018; 648:97–105.

https://doi.org/10.1016/j.gene.2018.01.051
PMID:29428128

40. Coomans de Brachène A, Demoulin JB. FOXO transcription factors in cancer development and therapy. Cell Mol Life Sci. 2016; 73:1159–72. https://doi.org/10.1007/s00018-015-2112-y PMID:26686861

41. Huang H, Tindall DJ. Dynamic FoxO transcription factors. J Cell Sci. 2007; 120:2479–87. https://doi.org/10.1242/jcs.001222 PMID:17646672

42. He Y, Wang C, Zhang X, Lu X, Xing J, Lv J, Guo M, Huo X, Liu X, Lu J, Du X, Li C, Chen Z. Sustained Exposure to *Helicobacter pylori* Lysate Inhibits Apoptosis and Autophagy of Gastric Epithelial Cells. Front Oncol. 2020; 10:581364. https://doi.org/10.3389/fonc.2020.581364 PMID:33194715

43. Deng Y, Zhang H. WITHDRAWN: Knockdown of lncRNA AK139128 alleviates cardiomyocyte autophagy and apoptosis of induced by myocardial hypoxia-reoxygenation injury via targeting miR-499/FOXO4 axis. Gene. 2019. [Epub ahead of print]. https://doi.org/10.1016/j.gene.2019.05.017 PMID:31075407

44. Bourgeois B, Madl T. Regulation of cellular senescence via the FOXO4-p53 axis. FEBS Lett. 2018; 592:2083–97. https://doi.org/10.1002/1873-3468.13057 PMID:29683489

45. Zhu M, Goetsch SC, Wang Z, Luo R, Hill JA, Schneider J, Morris SM Jr, Liu ZP. FoxO4 promotes early inflammatory response upon myocardial infarction via endothelial Arg1. Circ Res. 2015; 117:967–77. https://doi.org/10.1161/CIRCRESAHA.115.306919 PMID:26438688

46. Silhan J, Vacha P, Strnadova P, Vecer J, Herman P, Sulc M, Teisinger J, Obsilova V, Obsil T. 14-3-3 protein masks the DNA binding interface of forkhead transcription factor FOXO4. J Biol Chem. 2009; 284:19349–60. https://doi.org/10.1074/jbc.M109.002725 PMID:19416966

47. Sun X, Thorne RF, Zhang XD, He M, Li J, Feng S, Liu X, Wu M. LncRNA GUARDIN suppresses cellular senescence through a LRP130-PGC1α-FOXO4-p21-dependent signaling axis. EMBO Rep. 2020; 21:e48796. https://doi.org/10.15252/embr.201948796 PMID:32149459

48. de Keizer PL, Packer LM, Szypowska AA, Riedl-Polderman PE, van den Broek NJ, de Bruin A, Dansen TB, Marais R, Brenkman AB, Burgering BM. Activation of forkhead box O transcription factors by oncogenic BRAF promotes p21cip1-dependent senescence. Cancer Res. 2010; 70:8526–36. https://doi.org/10.1158/0008-5472.CAN-10-1563 PMID:20959475

49. Correction to: Unspliced XBP1 Confers VSMC Homeostasis and Prevents Aortic Aneurysm Formation via FoxO4 Interaction. Circ Res. 2018; 122:e66. https://doi.org/10.1161/RES.0000000000000204 PMID:29599281

50. Collier DM, Villalba N, Sackheim A, Bonev AD, Miller ZD, Moore JS, Shui B, Lee JC, Lee FK, Reining S, Kotlikoff MI, Nelson MT, Freeman K. Extracellular histones induce calcium signals in the endothelium of resistance-sized mesenteric arteries and cause loss of endothelium-dependent dilation. Am J Physiol Heart Circ Physiol. 2019; 316:H1309–22. https://doi.org/10.1152/ajpheart.00655.2018 PMID:30848676

51. Dai M, Yang B, Chen J, Liu F, Zhou Y, Zhou Y, Xu Q, Jiang S, Zhao S, Li X, Zhou X, Yang Q, Li J, et al. Nuclear-translocation of ACLY induced by obesity-related factors enhances pyrimidine metabolism through regulating histone acetylation in endometrial cancer. Cancer Lett. 2021; 513:36–49. https://doi.org/10.1016/j.canlet.2021.04.024 PMID:33991616

52. Dai X, Bu X, Gao Y, Guo J, Hu J, Jiang C, Zhang Z, Xu K, Duan J, He S, Zhang J, Wan L, Liu T, et al. Energy status dictates PD-L1 protein abundance and anti-tumor immunity to enable checkpoint blockade. Mol Cell. 2021; 81:2317–31.e6. https://doi.org/10.1016/j.molcel.2021.03.037 PMID:33909988

53. Ma Y, Zheng B, Zhang XH, Nie ZY, Yu J, Zhang H, Wang DD, Shi B, Bai Y, Yang Z, Wen JK. circACTA2 mediates Ang II-induced VSMC senescence by modulation of the interaction of ILF3 with CDK4 mRNA. Aging (Albany NY). 2021; 13:11610–28. https://doi.org/10.18632/aging.202855 PMID:33885378

SUPPLEMENTARY MATERIALS

Supplementary Figures

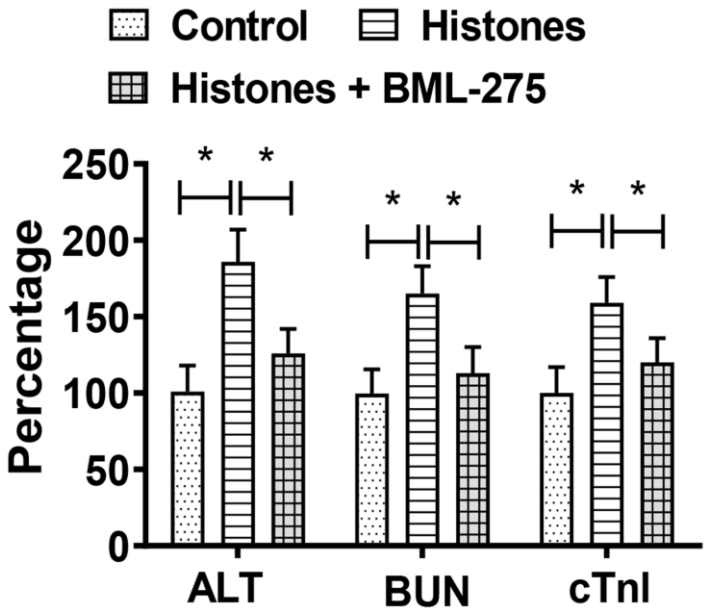

Supplementary Figure 1. ELISA detected the mount of organ injury markers in blood of mice. Changes of organ injury markers are presented as percentage by setting that without treatment as 100%. Means ± SD are presented; Student's *t*-test, $^{*}P < 0.05$ vs. the corresponding control.

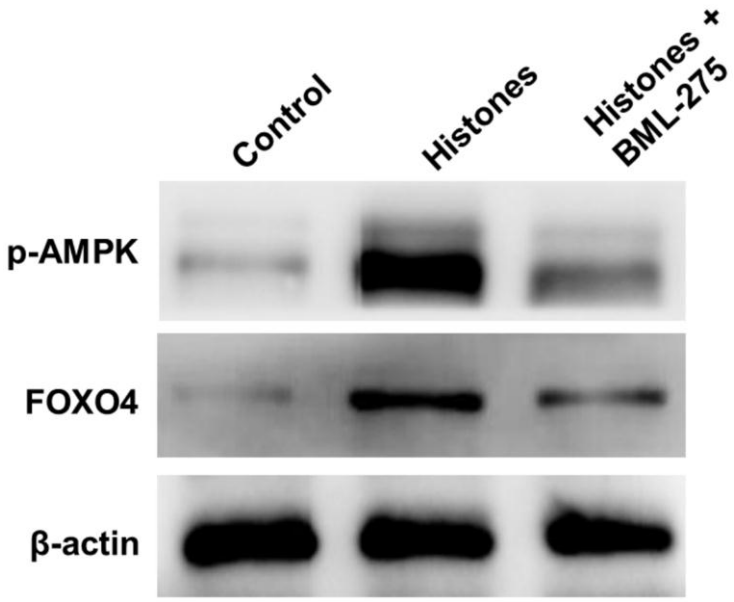

Supplementary Figure 2. Western blotting detected the AMPK/FOXO4 pathway proteins level vascular tissues of mice after histones or histones + BML-275 treatment.

Supplementary Table

Supplementary Table 1. Oligos used in the study.

Name	Sequcence 5′ to 3′	NCBI Reference Sequence	Posision in the mRNA (nt)
IL1β-F:	GCTCGCCAGTGAAATGATGG	NM_000576.3	From 105 to 434
IL1β-R	TCGTGCACATAAGCCTCGTT		
TNF-α-F	CACCACTTCGAAACCTGGGA	NM_000594.4	From 1030 to 1253
TNF-α-R	AGGAAGGCCTAAGGTCCACT		
IL-18-F	ATCGCTTCCTCTCGCAACAA	NM_001243211.2	From 156 to 378
IL-18-R	GAGGCCGATTTCCTTGGTCA		
NLRP3-F	CTGGCATCTGGGGAAACCT	NM_001079821.3	From 11 to 101
NLRP3-R	CTTAGGCTTCGGTCCACACA		
ASC-F	ATCCAGGCCCCTCCTCAG	NM_013258.5	From 368 to 557
ASC-R	AGAGCTTCCGCATCTTGCTT		
Caspase-1-F	ACATCCCACAATGGGCTCTG	NM_001223.5	From 991 to 1223
Caspase-1-R	TTCACTTCCTGCCCACAGAC		
ZBTB16-F	CCCTCCTCGGCTCTCGG	NM_001018011.3	From 12 to 209
ZBTB16-R	GGGTTCTGCAGCTGGATCAT		
HDAC1-F	ACTGCTAAAGTATCACCAGAGGG	NM_004964.3	From 573 to 940
HDAC1-R	CACACTTGGCGTGTCCTTTG		
FOXO4-F	GGGAAAAGGCCATTGAAAGCG	NM_001170931.2	From 842 to 982
FOXO4-R	TGTGGCGGATCGAGTTCTTC		
NFκB1-F	GGGCAGGAAGAGGAGGTTTC	NM_001165412.2	From 20 to 447
NFκB1-R	CTTCTGCCATTCTGAAGCCG		
NUPR1-F	ATGCCCACTTCACCTCTGAC	NM_001042483.2	From 197 to 272
NUPR1-R	CAGCTTCTCTCTTGGTGCGA		
NR1H4-F	GCAAAGAGATGGGAATGTTGGC	NM_001206977.2	From 1110 to 1598
NR1H4-R	CAGAATGCCCAGACGGAAGT		
TRIM25-F	CGCAAATGTTCCCAGCACAA	NM_005082.5	From 524 to 1382
TRIM25-R	GCACCTTGGCCTTGAGAGAT		
MYC-F	GCAATGCGTTGCTGGGTTAT	NM_001354870.1	From 37 to 330
MYC-R	CGCATCCTTGTCCTGTGAGT		
RNF4-F	GTTAGGAGGTCTGCGTCTGG	NM_001185009.3	From 5 to 190
RNF4-R	GTCAGCGGGGAACAAAAACC		
SUZ12-F	ACAAACATCAAAAGCTTGTCAGC	NM_001321207.2	From 613 to 827
SUZ12-R	AGGTCAGGATTCAAAGGCACC		
p16-F	CCGAATAGTTACGGTCGGAGG	NM_000077.5	From 151 to 499
p16-R	AATCGGGGATGTCTGAGGGA		
p21Cip1-F	AAGTCAGTTCCTTGTGGAGCC	NM_000389.5	From 20 to 129
p21Cip1-R	GCATGGGTTCTGACGGACAT		
p53-F	AATCTACTGGGACGGAACAGCTTTGAGG	NM_000546.6	From 929 to 1089
p53-R	GGAGAGGAGCTGGTGTTGTTGGG		
GAPDH-F	AATGGGCAGCCGTTAGGAAA	NM_001256799.3	From 58 to 225
GAPDH-R	GCGCCCAATACGACCAAATC		